Supplementary material accompanying "Long-time-scale transients in an industrial scale slurry pipeline near the laminar-turbulent transition"

Amitosh Dash[1] and Christian Poelma*[1]

[1]Multiphase Systems (Process & Energy), Mechanical, Maritime and Materials Engineering, Delft University of Technology, Mekelweg 2, 2628CD, Delft, The Netherlands
*Corresponding author. E-mail: c.poelma@tudelft.nl

Slurry characterization

The slurry sample is composed of Kaolin(ite) dispersed in tap water (electrical conductivity = 0.0635 S/m). In short, kaolin is a hydrophilic whitish powder with pseudo-hexagonal flakes (Murray, 1961, 2000). While there are several publications characterizing Kaolin, properties may vary from sample to sample and is likely to be dependent on the mineralogy as well. This makes characterization a necessary step.

We report information on particle sizing, mass density, rheology, zeta potential, and in-situ settling velocity of the slurry. The mass density and rheology measurements are based on slurry samples collected midway through an experimental day corresponding to the unaltered inflow experiments (wall sampling). All ex-situ tests presented here were performed at the Physical Laboratory located at Deltares.

Particle sizing

The particle size distribution of kaolin was determined using a Malvern Mastersizer 2000, which relies on a light scattering technique. A dilute sample of the slurry was stirred at 2000 rpm, strong enough to prevent agglomerates of clay particles. The results are presented in Figure 1(a). We show the distribution of samples from the pipeline (dispersed) and of the dry clay powder (undispersed). For the latter, measurements were made after one hour of continuous stirring in the measurement device. It is evident that the particles in the dispersed sample are finer than in the undispersed sample. There could be a couple of explanations for these: particles in the undispersed sample might still be stuck due to cohesive forces, while particles in the dispersed sample might have experienced attrition in the slurry pump. Of course, the dispersed sample is of higher interest, for which d_{10} = 1.18 μm, d_{50} = 5.18 μm, d_{90} = 20.76 μm. The particles are relatively fine by the standards of the slurry transport community (Pullum, Boger, and Sofra, 2018).

Mass density

The mass density of the slurry samples was estimated by three different techniques: drying-weighing, 25 ml glass beaker pycnometer, and a handheld density meter (Anton Paar DMA-35). We report results from all three techniques in Figure 1(b), but the drying-weighing technique is least prone to errors. The results of the handheld density meter were typically close to that from the drying-weighing method (except one instance). The mass densities estimated using the beaker pycnometer technique systematically overestimated densities by 2%. For the drying-weighing technique, a slurry sample is

allowed to dry in an oven at 105 °C for > 24 hours. By knowing the weights of the slurry sample before and after drying, the mass fraction can be determined. To convert the mass fraction of the slurry to mass density of the slurry, the mass density of individual Kaolin particles is necessary. This was determined to be 2695.2 kg/m^3 by an AccuPyc 1330 pycnometer. The density of the slurry is approximately 1152.1 kg/m^3. The measured mass densities across the samples collected during the "unaltered inflow" experiments reflect the (in)homogeneity of the flow when wall sampling was performed. The biggest deviations in the measured mass densities occur for 0.83 m/s ↓, 0.63 m/s ↓, and 0.60 m/s ↑, which are also the cases where peculiarities in the measured bulk velocities were observed **??**(a).

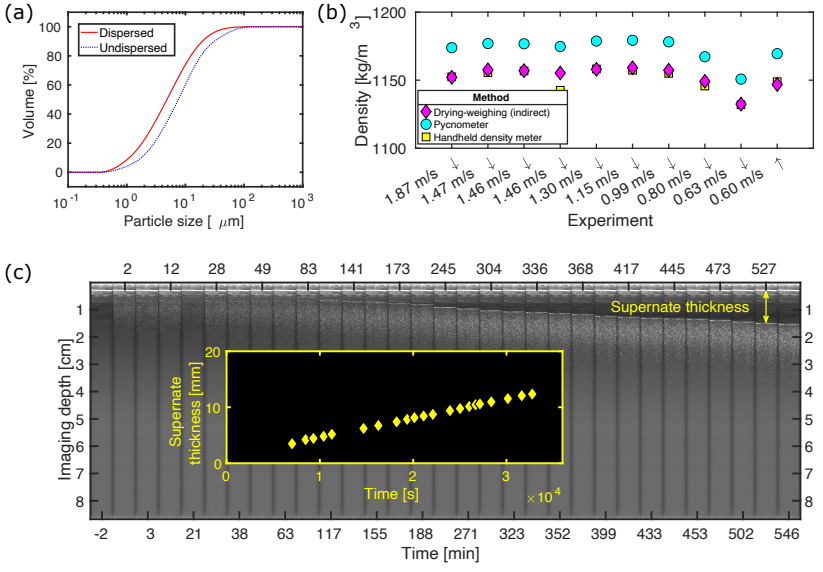

Figure 1: (a) Cumulative particle size distribution of the kaolin particles (b) Mass density for samples collected for the unaltered inflow experiments (c) In-situ settling of the slurry under quiescent conditions.

Rheology

In our case, this slurry is specifically used in order to mimic the rheological properties of wastewater, which is typically non-Newtonian, can exhibit a yield stress, and is shear thinning (Eshtiaghi *et al.*, 2013). Of course, in reality, actual wastewater will have even more complex properties such as thixotropy (history-dependent rheology).

For the purpose of this work, we describe the rheology of the slurry using a Herschel-Bulkley equation, $\tau = \tau_y + K\dot{\gamma}^n$. Here, τ is the shear stress and $\dot{\gamma}$ is the shear rate, which together determine the rheogram. To characterize the slurry, the following are needed: τ_y (yield stress), K (consistency index), and n (behaviour index). The apparent viscosity of the slurry, η, can then be determined as $\eta = \tau/\dot{\gamma}$.

Typically, two yield stresses are quantifiable - a static and a dynamic yield stress. The former would be the minimum stress needed to start a flow whereas the latter would be the minimum stress necessary to sustain a flow. For the present work, knowing the dynamic yield stress is more relevant. The static yield stress can be determined from steady shear rate measurements in which the shear rate is increased in time and the dynamic yield stress can be determined from steady shear rate measurements wherein the shear rate is decreased (Dinkgreve *et al.*, 2016).

Rheological characterization is performed using a HAAKE MARS I rheometer (Thermo Scientific, Germany) with a conventional bob-cup geometry. This simple geometry is sufficient as the slurry is thin and fluid-like. The temperature is set at 18°C.

Two different protocols were followed: one with controlled shear stress (CSS) followed by one with controlled shear rate (CSR). In CSS experiments, torque on the bob is controlled while in CSR experiments, torque on the bob is measured. Prior to performing each protocol, a fresh sample was agitated manually and added to a new cup.

In the CSS measurements, the shear stress is slowly ramped up from 0-2 N/m^2 over the course of 200 s in a linear, stepwise manner. Data is sampled every 2 s returning 100 points. The shear rate and apparent viscosity are measured. After the maximum shear stress is reached, the ramp direction is reversed immediately from 2-0 N/m^2 in a similar manner.

In the CSR measurements, the shear rate is slowly ramped up from 0-25 s^{-1} over 100 s in a linear, stepwise manner. Hereafter, the shear rate is ramped up from 25-300 s^{-1} over 200 s in a linear, stepwise manner. Data is sampled every 2 s returning 150 points. The shear stress and apparent viscosity are measured. After the maximum shear rate is reached, the ramp direction is immediately reversed from 300-0 s^{-1} in a similar manner.

Given the relatively low volumetric concentration of kaolin, the slurry has a low yield stress. Fitting the Herschel-Bulkley equation directly to CSR measurements will yield an "apparent" yield stress. Hence, a CSS measurement allows for an accurate estimation of a "true" yield stress, due to an improved resolution of shear stresses. This τ_y is then used in a recast Herschel-Bulkley equation, $\log(\tau - \tau_y) = \log K + n \log \dot{\gamma}$, in combination with CSR measurements to recover K, n.

In Figure 2, we present the rheology of the slurry sample collected during the turbulent flow measurements. Based on the rheograms in Figure 2(a, b), corresponding to the CSR protocols, it can be seen that the apparent yield stress is in the order of 1 Pa. Moreover, there are no discernible differences between the ramp-up and ramp-down portions of the protocol, suggesting the absence of any significant thixotropic behaviour. However, on the logarithmic scale, it is evident that there are not enough data points for the low shear rates, that would be necessary for one to confidently estimate the yield stress.

The CSS measurements, thus, solve this issue, as is evident in Figure 2(d). The rheogram can be reformulated to plot the apparent viscosity as a function of shear stress, like in Figure 2(c). For the ramp-up measurements, there are two shear stresses at which a sharp drop in the apparent viscosity is observed, at approximately 0.6 Pa and 0.85 Pa. The former might be related to slip between the slurry and the bob and is not of physical interest. The latter represents the desired yield stress that can be used to characterize the slurry. Similar two-step yielding behaviour has been observed for mud suspensions (see Shakeel, Kirichek, and Chassagne, 2020, Figure 4 therein). For the ramp-down measurement, there is only a single shear stress at which there is a sharp change in viscosity, at approximately 0.9 Pa. We use the ramp-down segment to estimate τ_y. Using this value from the CSS measurement, we use the ramp-down portion of the CSR rheogram to determine K, n. In short, we determine the following properties for this slurry: $\tau_y = 0.8889$ Pa, $K = 0.1579$ Pa·$s^{0.4579}$, $n = 0.4579$.

Zeta potential

Kaolin is also considered to have "relatively weak cohesive properties" (Baas, Best, and Peakall, 2016). We confirm this by measuring the zeta potential with a Malvern ZetaNano device. In short, this measurement indicates the surface charge of the particles and their ability to attract/repel each other. Prior to measuring the zeta potential, the slurry was diluted with supernatant (carrier fluid) from the flow facility. The zeta potential was measured to be -18.7 ± 0.469 mV. This value suggests that flocculation should not occur readily, and that the slurry is relatively stable. If flocculation is present, settling velocities would be enhanced.

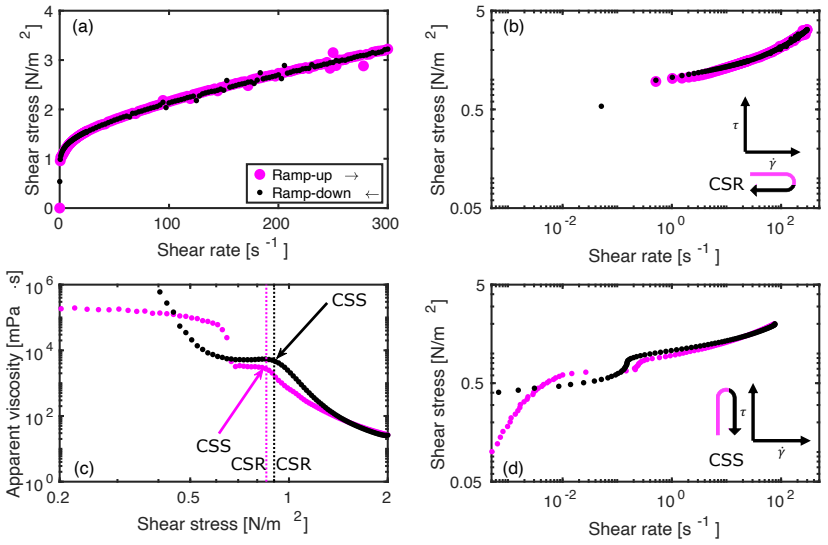

Figure 2: Rheology of the sample collected under turbulent conditions. (a), (b) CSR rheogram on linear and log scales (c) Apparent viscosity from CSS measurement (d) CSS rheogram on log scale.

Settling test

Another common test to characterize sediment/slurry is to perform a batch settling test, in order to estimate a settling velocity. We perform this in-situ in the horizontal pipe section of the industrial scale facility. After homogenizing the flow, the flow is stopped, and ultrasound images of the slurry are taken from the upper section of the horizontal pipe section, similar as those shown in Figure 1(c). Images are taken at irregular intervals. When no images are being recorded, the ultrasound power is reduced to a minimum to minimize its influence on the slurry. Based on the slurry "blanket" height or thickness of the supernate measured under quiescent conditions over several hours (similar to Locatelli *et al.*, 2015), the settling velocity of this slurry is estimated to be 342 nm/s or 1.2 mm/hour. These values might be affected by the polydispersity of the slurry. Imaging from top will likely capture the finer particles, while imaging from the bottom will focus on the coarser particles.

Relevant equations for laminar and turbulent flows of a non-Newtonian slurry

We reproduce a few relevant equations/models from the summary compiled by van den Heever, Sutherland, and Haldenwang (2014). Please note that we only reproduce those equations/models that are used in the main text to compare with our measured data. Typically, relations are obtained between the bulk velocity, U_b, the wall shear stress, τ_w, the pipe diameter, D, and the slurry rheology, τ_y, K, n.

Laminar flow calculations

Under the absence of slip, the equation for volumetric flow rate can be combined with the Herschel-Bulkley rheological model to yield Equation (1). This equation provides a relation between the pseudo shear rate, the wall shear stress and the slurry rheology. This equation is analytically accurate and does not involve any major assumptions.

$$\frac{8U_b}{D} = \left(\frac{1}{K}\right)^{1/n} \frac{4}{\tau_w^3}(\tau_w - \tau_y)^{(n+1)/n} \times \left[\frac{n\tau_w^2}{(n+1)} - \frac{2n^2\tau_y(\tau_w - \tau_y)}{(n+1)(2n+1)} - \frac{2n^2(\tau_w - \tau_y)^2}{(n+1)(3n+1)}\right] \quad (1)$$

Turbulent flow model of Wilson and Thomas

A model to predict the turbulent flow of a non-Newtonian fluid was developed by Wilson and Thomas (1985) and Thomas and Wilson (1987). While the model was first presented in Wilson and Thomas (1985), a plus sign was incorrectly written as a minus sign (Thomas, 2018). This was rectified in Thomas and Wilson (1987). This model focuses on the change of the velocity profile in the wall region ("viscous layer thickening"). Equation (2) shows how the bulk velocity can be estimated.

$$U_b = 2.5u_* \ln\left(\frac{D\rho u_*}{\mu'}\right) + u_*[11.6(\alpha - 1) - 2.5\ln(\alpha) - \Omega] \quad (2)$$

The term u_* is the shear velocity ($= \sqrt{\tau_w/\rho}$). The term α is the ratio of areas under the non-Newtonian and assumed Newtonian flow curves at a given wall shear stress. The term μ' is the apparent viscosity at the wall shear stress. The term Ω accounts for blunting of the velocity profile near the pipe centerline. The equations for α and Ω are given in Equation (3) and Equation (4) respectively.

$$\alpha = 2\left[\frac{1 + n(\frac{\tau_y}{\tau_w})}{(1+n)}\right] \quad (3)$$

$$\Omega = -2.5\ln\left[1 - \left(\frac{\tau_y}{\tau_w}\right)\right] - 2.5\left(\frac{\tau_y}{\tau_w}\right)\left[1 + 0.5\left(\frac{\tau_y}{\tau_w}\right)\right] \quad (4)$$

Turbulent flow model of Slatter

Another model was developed by Slatter (1995) for turbulent flow of non-Newtonian slurries. Basically, it relies on the classical roughness function utilized for Newtonian flows. But, it replaces the roughness with a characteristic particle size, d_{85}. Using this, a roughness Reynolds number, R_r. Equation (5) shows how this is defined for a Herschel-Bulkley fluid.

$$R_r = \frac{8\rho u_*^2}{\tau_y + K(\frac{8u_*}{d_{85}})^n} \quad (5)$$

Depending on the value of the roughness Reynolds number, the flow can be classified as either "smooth wall turbulent flow" or "rough wall turbulent flow". The critical roughness Reynolds number is 3.32. According to the scenario, the appropriate relation can be used: Equation (6) for smooth or Equation (7) for rough.

$$U_b = u_*\left[2.5\ln\left(\frac{D}{2d_{85}}\right) + 2.5\ln R_r + 1.75\right] \quad \text{for} \quad R_r \leq 3.32 \quad (6)$$

$$U_b = u_*\left[2.5\ln\left(\frac{D}{2d_{85}}\right) + 4.75\right] \quad \text{for} \quad R_r > 3.32 \quad (7)$$

Bibliography

Baas, J. H., Best, J. L., and Peakall, J., *"Comparing the transitional behaviour of kaolinite and bentonite suspension flows,"* Earth Surface Processes and Landforms **41**, 1911–1921 (2016).

Dinkgreve, M., Paredes, J., Denn, M. M., and Bonn, D., *"On different ways of measuring âĂIJtheâĂİ yield stress,"* Journal of Non-Newtonian Fluid Mechanics **238**, 233–241 (2016).

Eshtiaghi, N., Markis, F., Yap, S. D., Baudez, J.-C., and Slatter, P., *"Rheological characterisation of municipal sludge: a review,"* Water Research **47**, 5493–5510 (2013).

van den Heever, E., Sutherland, A., and Haldenwang, R., *"Influence of the rheological model used in pipe-flow prediction techniques for homogeneous non-Newtonian fluids,"* Journal of Hydraulic Engineering **140**, 04014059 (2014).

Locatelli, F., François, P., Laurent, J., Lawniczak, F., Dufresne, M., Vazquez, J., and Bekkour, K., *"Detailed velocity and concentration profiles measurement during activated sludge batch settling using an ultrasonic transducer,"* Separation Science and Technology **50**, 1059–1065 (2015).

Murray, H. H., *"Industrial applications of kaolin,"* Clays and Clay Minerals **10**, 291–298 (1961).

Murray, H. H., *"Traditional and new applications for kaolin, smectite, and palygorskite: a general overview,"* Applied Clay Science **17**, 207–221 (2000).

Pullum, L., Boger, D. V., and Sofra, F., *"Hydraulic mineral waste transport and storage,"* Annual Review of Fluid Mechanics **58**, 157–185 (2018).

Shakeel, A., Kirichek, A., and Chassagne, C., *"Rheological analysis of natural and diluted mud suspensions,"* Journal of Non-Newtonian Fluid Mechanics **286**, 104434 (2020).

Slatter, P. T., *Transitional and turbulent flow of non-Newtonian slurries in pipes*, Ph.D. thesis, University of Cape Town (1995).

Thomas, A. D., *"Some observations regarding non-Newtonian turbulent flow and transition, especially in relation to the Wilson–Thomas (1985) theory,"* in *Paste 2018: Proceedings of the 21st International Seminar on Paste and Thickened Tailings* (Australian Centre for Geomechanics, 2018) pp. 205–216.

Thomas, A. D., and Wilson, K. C., *"New analysis of non-newtonian turbulent flow – yield-power-law fluids,"* The Canadian Journal of Chemical Engineering **65**, 335–338 (1987).

Wilson, K. C., and Thomas, A. D., *"A new analysis of the turbulent flow of non-newtonian fluids,"* The Canadian Journal of Chemical Engineering **63**, 539–546 (1985).

Cite this article: Dash, A., & Poelma, C. (2022). Supplementary material accompanying "Long-time-scale transients in an industrial scale slurry pipeline near the laminar-turbulent transition". *Flow*, *0*, . doi:10.4153/xxxx